Publications of the Korean Astronomical Society
27: 187 ∼ 193, 2012 September

ISSN 1225-1534 (Print)
http://dx.doi.org/10.5303/PKAS.2012.27.4.187

AKARI OBSERVATIONS OF THE INTERSTELLAR MEDIUM

Takashi Onaka
Department of Astronomy, Graduate School of Science, The University of Tokyo, Tokyo 113-0033, Japan
E-mail: onaka@astron.s.u-tokyo.ac.jp
(Received June 28, 2012; Accepted July 23, 2012)

ABSTRACT

AKARI has 4 imaging bands in the far-infrared (FIR) and 9 imaging bands that cover the near-infrared (NIR) to mid-infrared (MIR) contiguously. The FIR bands probe the thermal emission from sub-micron dust grains, while the MIR bands observe emission from stochastically-heated very small grains and the unidentified infrared (UIR) band emissions from carbonaceous materials that contain aromatic and aliphatic bonds. The multi-band characteristics of the *AKARI* instruments are quite efficient to study the spectral energy distribution of the interstellar medium, which always shows multi-component nature, as well as its variations in the various environments. *AKARI* also has spectroscopic capabilities. In particular, one of the onboard instruments, Infrared Camera (IRC), can obtain a continuous spectrum from 2.5 to 13 μm with the same slit. This allows us to make a comparative study of the UIR bands in the diffuse emission from the 3.3 to 11.3 μm for the first time. The IRC explores high-sensitivity spectroscopy in the NIR, which enables the study of interstellar ices and the UIR band emission at 3.3–3.5 μm in various objects. Particularly, the UIR bands in this spectral range contain unique information on the aromatic and aliphatic bonds in the band carriers. This presentation reviews the results of *AKARI* observations of the interstellar medium with an emphasis on the observations of the NIR spectroscopy.

Key words: infrared: ISM; ISM: general; ISM: dust

1. INTRODUCTION

The interstellar medium (ISM) emits a significant fraction of its energy at infrared wavelengths either as the dust continuum or as the line emission from gas species. Infrared observations are thus a powerful tool to investigate the nature of the interstellar medium. The dust emission in the infrared consists at least of three components: far-infrared (FIR) thermal emission of sub-micron grains, mid-infrared continuum emission coming from very small grains that are stochastically heated, and the unidentified infrared (UIR) bands in the near- to mid-infrared (NIR to MIR) originating from polycyclic aromatic hydrocarbons (PAHs) or related materials (e.g., Li & Draine, 2001; Tielens, 2008). To investigate the properties of dust emission properly, therefore, it is crucial to cover a wide spectral range of the infrared contiguously.

The Japanese infrared satellite, *AKARI*, launched in 2006 February (Murakami et al., 2007), was equipped with two onboard instruments: the Far-Infrared Surveyor (FIS: Kawada et al., 2007) and the Infrared Camera (IRC: Onaka et al., 2007). They cover the NIR to FIR spectral range with 13 imaging bands contiguously, which enables detailed studies of the ISM in various objects. The FIS 4 bands in the FIR clearly delineate the presence of active star-forming regions and cold ISM separately in galaxies (Suzuki et al., 2010), while the 7 μm (S7) band of the IRC fully covers the strong UIR bands at 6.2 and 7.7 μm and thus is efficient in tracing the UIR band emission even in faint regions, such as the outflow from the galactic disk (Onaka et al., 2010a).

Both the FIS and IRC also have spectroscopic capabilities, which are useful to study the physical properties of the gas and dust. The imaging Fourier transform

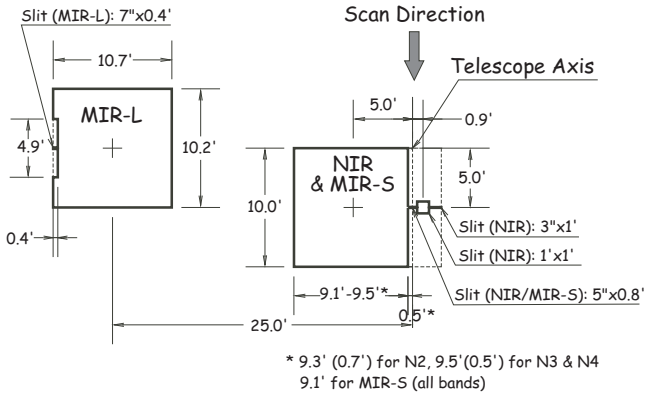

Fig. 1. Field-of-view configuration of the IRC (Onaka et al., 2007). The NIR and MIR-S channels share the same field-of-view by means of the beam splitter.

spectrometer of the FIS (Murakami et al., 2010) offers a unique opportunity to investigate the distribution of several emission lines and dust bands simultaneously in various extended objects (Yasuda et al., 2009; Okada et al., 2010; Kawada et al., 2011; Kaneda et al., 2012).

The IRC has the capability to perform slit-less spectroscopy from the NIR to MIR, which facilitates efficient spectroscopic surveys in the infrared (e.g., Shimonishi et al., 2008). The IRC slit spectroscopy also enables us to obtain a continuous spectrum from 2.5 to 13 μm with the same region (Ohyama et al., 2007) and thus to make a comparative study of the UIR bands in the diffuse emission from the 3.3 to 11.3 μm for the first time (Mori et al., 2012). Furthermore, NIR spectroscopy maintains its high sensitivity even in the warm mission phase (Onaka et al., 2010b) although the spectral resolution is rather low ($\sim$ 100 with the grism). It provides significant information on the various ice species (Shimonishi et al., 2010; Aikawa et al., 2012) and on the UIR band emission at 3.3–3.5 μm in a variety of objects (Boulanger et al., 2011; Kaneda et al., 2012; Ohsawa et al., 2012). In particular, the UIR bands in this spectral range contain unique information on the aromatic and aliphatic bonds in the band carriers (Kwok & Zhang, 2011; Jones, 2012).

The following section focuses on observations of the IRC NIR spectroscopy of the ISM taken as part of the mission program of *AKARI* ISM in our Galaxy and nearby galaxies (ISMGN; Kaneda et al., 2009).

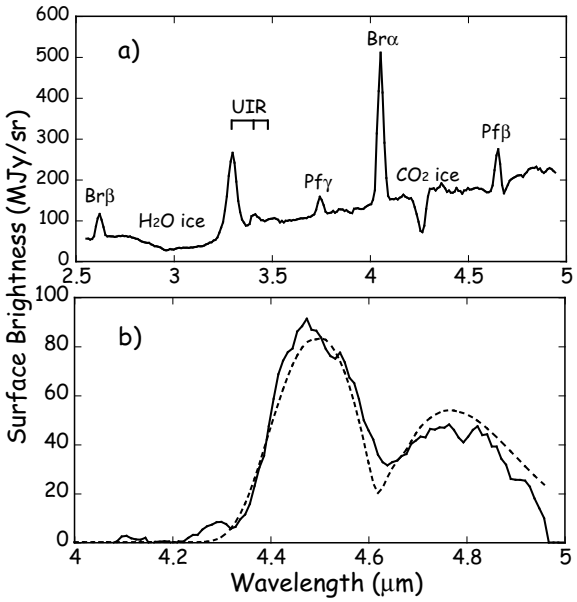

Fig. 2. Examples of the IRC NIR slit spectra. (a) spectrum of the diffuse emission of the Galactic plane and (b) IRC spectrum of a knot in Cas A supernova remnant (Rho et al., 2012). Model calculation of CO gas emission is also plotted by the dashed line.

2. IRC NEAR-INFRARED SPECTROSCOPY

The IRC consists of three channels: NIR, MIR-S, and MIR-L (Onaka et al., 2007). Figure 1 shows the focal-plane configuration of the IRC. Each channel has a small slit area, which is used for the spectroscopy of diffuse emission. The NIR and MIR-S channels share the same field-of-view by means of the beam splitter and thus the spectrum of the same area can be obtained from 2.5 to 13 μm contiguously. The NIR channel works even after the exhaustion of the liquid helium, owing to the onboard cryocooler. It facilitates high-sensitivity spectroscopy in the 2–5 μm region, which has not been possible with past instruments. In fact, this spectral range contains several important gas lines and dust bands. Examples of the IRC NIR slit spectra are shown in Figure 2. Figure 2 (a) shows a slit spectrum of a target in the Galactic plane, which shows hydrogen recombination lines at 2.626, 3.297, 3.741, 4.052, and 4.654 μm, H_2O and CO_2 ice absorption at 3.0 and 4.3 μm, and the UIR band emission at 3.3–3.5 μm. Figure 2 (b) shows the spectrum of a knot in Cas A supernova remnant that shows CO gas emission at 4.4–4.8 μm (Rho et al., 2012). A number of molecular hydrogen lines are also detected in this special range

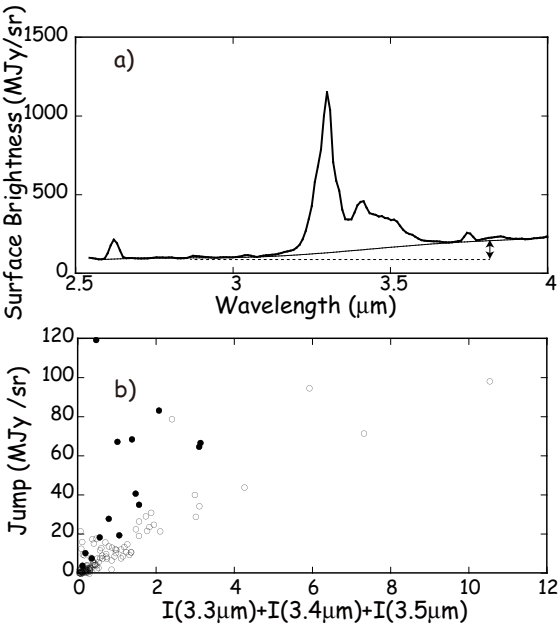

Fig. 3. (a) Example of the IRC NIR spectrum of the diffuse emission toward the Galactic plane. The jump in the NIR continuum is indicated by the arrow. (b) The jump strength in MJy sr^{-1} vs. the summation of the 3.3–3.5 μm UIR band intensities for the Galactic plane targets. The filled circles indicate sources with the CO_2 ice absorption at 4.3 μm.

(Lee et al., 2011). In the following, some results of IRC observations of the UIR bands in the diffuse emission are presented.

2.1. SPECTRUM OF THE GALACTIC PLANE

We obtain NIR spectra towards more than 100 positions in the Galactic plane with the NIR grism mode of the IRC. An example of the spectrum in the 3 μm region is shown in Figure 3 (a). The spectrum clearly shows the presence of the UIR band emission at 3.3, 3.4, and 3.5 μm. The 3.4 μm band is thought to come from aliphatic bonds (Kwok & Zhang, 2011) or higher excitation bands (Allamandola et al., 1989). The 3.5 μm is known to consist of more than one components, but they are not resolved with the resolution of the present grism spectroscopy. In addition to the band emission, there is a difference or a jump in the continuum level across the 3 μm UIR bands as indicated by the arrow (Boulanger et al., 2011), which may be attributable to the recurrent (Poincaré) fluorescence (Legèr et al., 1988) or the combination bands.

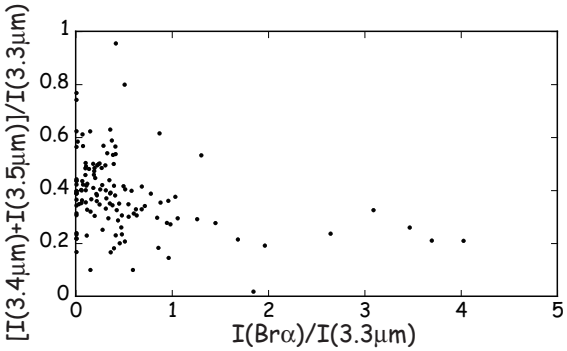

Fig. 4. The ratio of the summation of the UIR 3.4 and 3.5 μm band intensity to the UIR 3.3 μm band intensity vs. the Brα to the 3.3 μm band intensity ratio for the Galactic plane targets.

To confirm that the jump is associated with the UIR band emission, Figure 3 (b) plots the jump strength estimated from the difference between the continuum at 3.0 and 3.7 μm in MJy sr^{-1} against the summation of the UIR 3.3, 3.4, and 3.5 μm band intensities for the Galactic plane targets. Except for those with the CO_2 ice absorption at 4.3 μm (filled circles), a good correlation is seen, supporting that the jump is associated with the UIR band carriers. The CO_2 ice absorption should be associated with the H_2O absorption at 3.0 μm, which is not corrected for, and thus the jump strength may be overestimated for those targets.

Figure 4 shows the plot of the ratio of the summation of the UIR 3.4 and 3.5 μm bands to the UIR 3.3 μm band intensity against the ratio of Brα to the 3.3 μm band intensity for the Galactic plane targets. It indicates that the spectra toward the region with ionized gas show weaker 3.4 and 3.5 μm bands, suggesting that aliphatic bonds may be reduced in the ionized gas or that the band carriers are processed in the ionized gas.

2.2. DEUTERATED PAH FEATURES

FUSE observations indicate that the interstellar deuterium is depleted compared to the prediction of the chemical evolution model and the depleted deuterium may be trapped in interstellar grains (Linsky et al., 2006). Draine (2006) proposes that the depleted deuterium resides in PAHs and suggests that the D/H in PAHs could be as high as 30%. The 3.3 and 3.4 μm bands are predicted to shift to around 4.4 and 4.6 μm, respectively, for deuterated PAHs. Peeters et al. (2004) report possible detection of deuterated PAH bands at

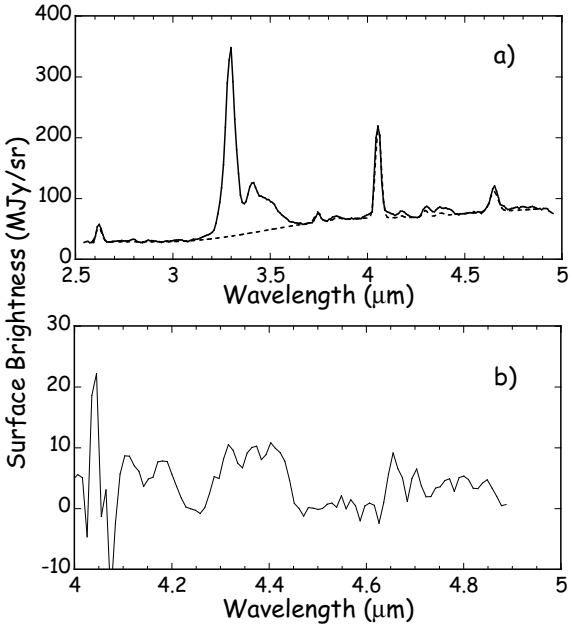

Fig. 5. (a) IRC spectrum of M17. The dotted line indicates the ionized gas emission spectrum to be subtracted. (b) Residual spectrum of the M17 spectrum after the ionized gas contribution has been subtracted. Note that the scale of (b) is enlarged compared to (a).

the Orion bar and M17 and suggest that the ratio of the total intensity of the 4 μm bands to that of the 3 μm bands is 17 and 36%, respectively. However, the detection is in a 4σ level even for the best case and thus needs further observations for confirmation.

We obtain NIR spectra of the Orion bar and M17 with the IRC and search for band emission in the 4.3–4.7 μm region. The IRC spectrum of M17 is shown in Figure 5 (a). There may be slight excess emission around 4.4 μm, where a weak HI recombination line overlaps at 4.37 μm. The 4.65 μm region is dominated by strong Pfβ emission. The contribution of the ionized gas is estimated from the spectrum taken at a different slit position (dashed line), where the line emission from ionized gas is dominant, and is subtracted from the spectrum. It should be noted that the observed recombination line intensities agree well with the model predictions with the Case B condition. The residual spectrum is shown in Figure 5 (b), which indicates small excess emission around 4.3 and 4.7 μm. Compared to the total UIR band intensities in the 3 μm region, the excess emission in 4.3–4.7 μm is estimated as 3%. The spectrum of the Orion bar gives a similar result.

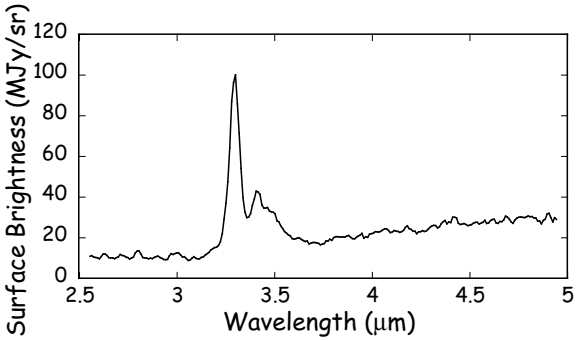

Fig. 6. IRC spectrum of the Galactic plane that is not associated with the ionized gas.

Since the contribution of the ionized gas gives an uncertainty in the estimated intensity of possible features at 4.3–4.7 μm, we search for spectra that do not show recombination line emissions. Figure 6 shows an example. It does not show any features in 4.3–4.7 μm, giving an upper limit of the features as 3% of the total 3 μm UIR band intensities.

The present IRC observations show that the deuterated PAH features in the 4 μm region are, if any, at most 3% of the total 3 μm band intensities, which is much smaller than the model prediction. However it is difficult to draw a definite conclusion on the presence of deuterated PAHs or the depletion of interstellar deuterium since here we simply compare the total band intensities of the 3 and 4 μm regions. The intensity of the emission bands depends not only on the abundance of the carriers, but also on the excitation conditions, which should be different at different bands, and also on the oscillator strengths, which can be different for vibration modes of molecules with different isotopes. The 3 and 4 μm band emission is thought to come from the smallest band carriers (e.g., Mori et al., 2012). Deuterated carriers could be large in size, which do not emit band emission dominantly at 3–4 μm. Finally it should be noted that further investigations are needed to attribute the possible excess emission seen in the residual spectrum, even if it is real, to deuterated band carriers.

3. WARM DEBRIS DISKS

In this section, one of the results based on the IRC all-sky survey (Ishihara et al., 2010), search for debris disks, is briefly described since only a few reports related to this topic are presented in this conference.

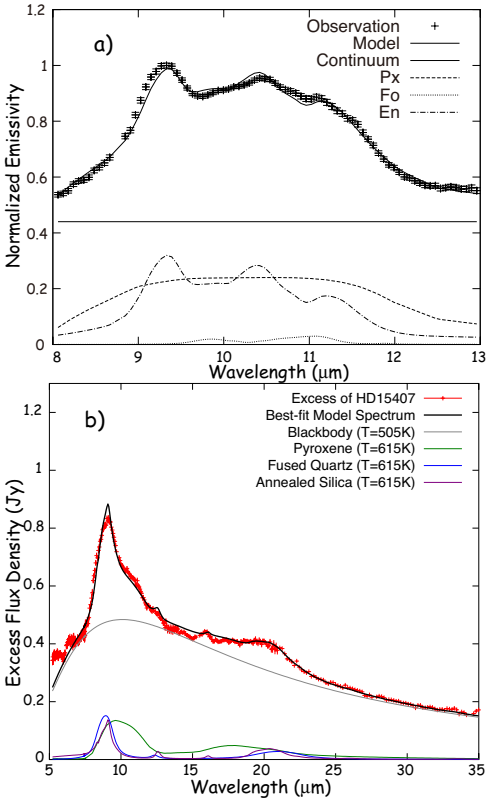

Fig. 7. IRS spectrum and decomposition of the dust components (a) HD165014 and (b)HD15407. See Fujiwara et al. (2010, 2012) for details.

The IRC all-sky survey provides high-sensitivity and high-spatial resolution data at 9 and 18 μm compared to the IRAS all-sky survey. Search for debris disks around main-sequence stars that show excess emission at 18 μm is carried out using the Tyco-2 spectral catalog and the 2MASS database (Fujiwara et al., 2012b). 24 debris disk candidates, of which 8 are new, are found in the search. Debris disks found in the IRAS survey are those with excess emission at 60 μm. Compared to them, the present search detects excess at a shorter wavelength and thus is biased to warmer debris disks, while having a more direct link to the planet formation region. In fact, follow-up observations with *Spitzer* and ground-based telescopes show interesting results. Figure 7 shows IRS spectra of two of the warm debris candidates (Fujiwara et al., 2010; 2012a). Both spectra show dust emission with fine structures. The spectrum of HD165014 (a) can be well fitted predominantly with enstatite ($MgSiO_3$) and that of HD15407 (b) shows silica (SiO_2) features clearly, both of which are distinctly different from the commonly seen forsterite (Mg_2SiO_4) features. Formation of both minerals requires the presence of large differentiated rocky bodies in the system. The results suggest that the warm debris disk constitutes its own class and deserves further investigations.

4. SUMMARY

AKARI has multi-band imaging and spectroscopic capabilities from NIR to FIR. It covers most of the emission from the ISM contiguously and thus provides an ideal opportunity to study the ISM in our Galaxy and galaxies in detail. In particular the NIR spectroscopy enables us to explore this spectral range with high sensitivity for the first time. The spectral range 2–5 μm contains several important lines and bands of gas and dust species. H_2O and CO_2 ices as well as H_2 gas can be most efficiently studied in this spectral range. The NIR UIR bands contain information on the aromatic and aliphatic bonds in carbonaceous dust, which cannot be investigated at other wavelengths. The *AKARI* all-sky survey also provides a significant database for the study of the ISM. This paper focuses on the results of the IRC NIR spectroscopy as well as the one based on the IRC all-sky survey, but there are a number of investigations on the ISM that cannot be discussed here or are still in progress. Most of the *AKARI* data are now open to the public and much more interesting results are anticipated to appear in the near future.

ACKNOWLEDGEMENTS

This work is based on observations with *AKARI*, a JAXA project with the participation of ESA. The author thanks all the members of the *AKARI* project and the members of the ISMGN team for their continuous help and encouragements. He also thanks F. Boulanger and C. Joblin for the useful discussions. This work is supported in part by a Grant-in-Aid from Japan Society for the Promotion of the Science.

REFERENCES

Aikawa, Y., et al., 2012, AKARI Observations of Ice Absorption Bands towards Edge-on Young Stellar Objects, A&A, 538, A57

Allamandola, L. J., Tielens, A. G. G. M., & Barker, J. R., 1989, Interstellar Polycyclic Aromatic Hydrocarbons – The Infrared Emission Bands, the Excitation/Emission Mechanism, and the Astrophysical Implications, ApJS, 71, 733

Boulanger, F., Onaka, T., Pilleri, P., & Joblin, C., 2011, Near-infrared Spectroscopy of Interstellar Dust, EAS Publ. ser., 46, 399
Draine, B. T., 2006, Can Dust Explain Variations in the D/H Ratio?, ASP Conf. ser., 348, 58
Fujiwara, H., et al., 2010, Enstatite-rich Warm Debris Dust Around HD165014, ApJ, 714, L152
Fujiwara, H., et al., 2012a, Silica-rich Bright Debris Disk around HD15407A, ApJ, 749, L29
Fujiwara, H., et al., 2012b, AKARI/IRC 18 μm Survey of Warm Debris Disks, submitted to A&A
Ishihara, D., et al., 2010, The AKARI/IRC Mid-infrared All-sky Survey, A&A, 514, A1
Jones, A., 2012, Variations on a Theme - the Evolution of Hydrocarbon Solids. II. Optical Property Modelling - the optEC(s) Model, A&A, 540, A2
Kaneda, H., Koo, B.-C., Onaka, T., & Takahashi, H., 2009, AKARI Observations of the ISM in our Galaxy and Nearby Galaxies, Adv. Sp. Res., 44, 1038
Kaneda, H., et al. 2012, Processing of Polycyclic Aromatic Hydrocarbons in Molecular-loop Regions near the Galactic Center Revealed by AKARI, PASJ, 64, 25
Kaneda, H., Yasuda, A., Onaka, T., Kawada, M., Murakami, N., Nakagawa, T., Okada, Y., & Takahashi, H., 2012, Properties of Dust in the Galactic Center Region Probed by AKARI Far-infrared Spectral Mapping - Detection of a Dust Feature, A&A, in press
Kawada, M., et al., 2007, The Far-Infrared Surveyor (FIS) for AKARI, PASJ, 59S, 389
Kawada, M., et al., 2011, Widely Extended [OIII] 88 μm Line Emission around the 30 Doradus Region Revealed with AKARI FIS-FTS, PASJ, 63, 903
Kwok, S. & Zhang, Y., 2011, Mixed Aromatic-aliphatic Organic Nanoparticles as Carriers of Unidentified Infrared Emission Features, Nature, 479, 80
Lee, H. -G., Moon, D. -S., Koo, B. -C., Onaka, T., Jeong, W. -S., Shinn, J. -H., & Sakon, I., 2011, Far-infrared Luminous Supernova Remnant Kes 17, ApJ, 740, 31
Legèr, A., D'Hendecourt, L., & Boissel, P., 1988, Predicted Fluorescence Mechanism in Highly Isolated Molecules – The Poincaré Fluorescence, PhRvL, 60, 921
Li, A. & Draine, B. T., 2001, Infrared Emission from Interstellar Dust. II. The Diffuse Interstellar Medium, ApJ, 554, 778
Linsky, J., et al., 2006, What Is the Total Deuterium Abundance in the Local Galactic Disk?, ApJ, 647, 1106
Mori, T. I., Sakon, I., Onaka, T., Kaneda, H., Umehata, H., & Ohsawa, R., 2012, Observations of the Near- to Mid-infrared Unidentified Emission Bands in the Interstellar Medium of the Large Magellanic Cloud, ApJ, 744, 68
Murakami, H., et al., 2007, The Infrared Astronomical Mission AKARI, PASJ, 59S, 369
Murakami, N., et al., 2010, Calibration of the AKARI Far-Irnfared Imaging Fourier-Transform Spectrometer, PASJ, 62, 1155
Ohsawa, R., et al., 2012, Investigation of PAHs in Galactic Planetary Nebulae with the AKARI/IRC and the Spitzer/IRS, this volume
Ohyama, Y., et al., 2007, Near-infrared and Mid-infrared Spectroscopy with the Infrared Camera (IRC) for AKARI, PASJ, 59S, 411
Okada, Y., et al., 2010, Properties of Active Galactic Star-Forming Regions Probed by Imaging Spectroscopy with the Fourier Transform Spectrometer (FTS) onboard AKARI, A&A, 514, 13
Onaka, T., et al., 2007, The Infrared Camera (IRC) for AKARI – Design and Imaging Performance, PASJ, 59S, 401
Onaka, T., Matsumoto, H., Sakon, I., & Kaneda, H., 2010a, Detection of the Unidentified Infrared Bands in a Hα Filament in the Dwarf Galaxy NGC1569 with AKARI, A&A, 514, A15
Onaka, T., et al., 2010b, AKARI Warm Mission, Proc. of SPIE, 7731, 77310M
Peeters, E., Allamandola, L. J., Bauschlicher, C. W., Jr., Hudgins, D. M., Sandford, S. A., & Tielens, A. G. G. M., 2004, Deuterated Interstellar Polycyclic Aromatic Hydrocarbons, ApJ, 604, 252
Rho, J., Onaka, T., Cami, J., & Reach, W. T., 2012, Spectroscopic Detection of Carbon Monoxide in the Young Supernova Remnant Cassiopeia A, ApJ, 747, L6
Shimonishi, T., Onaka, T., Kato, D., Sakon, I., Ita, Y., Kawamura, A., & Kaneda, H., 2008, AKARI Near-Infrared Spectroscopy: Detection of H_2O and CO_2 Ices toward Young Stellar Objects in the Large Magellanic Cloud, ApJ, 686, L99
Shimonishi, T., Onaka, T., Kato, D., Sakon, I., Ita, Y., Kawamura, A., & Kaneda, H., 2010, Spectroscopic Observations of Ices around Embedded Young Stellar Objects in the Large Magellanic Cloud with AKARI, A&A, 514, A12

Suzuki, T., Kaneda, H., Onaka, T., Nakagawa, T., & Shibai, H., 2010, Kiloparsec-scale Star Formation Law in M81 and M101 Based on AKARI Far-infrared Observations, A&A, 521, A48

Tielens, A. G. G. M., 2008, Interstellar Polycyclic Aromatic Hydrocarbon Molecules, ARA&A, 46, 289

Yasuda, A., et al., AKARI Far-Infrared Spectroscopic Observations of the Galactic Center Region, PASJ, 61, 511